IMPACT OF ISLSCP-II INITIATIVE GLOBAL SOIL WATER STORAGE CAPACITY OF THE ROOTING ZONE DATA ON T80 GCM

M. Ravindranath and G.R.Iyengar
Scientist-D Scientist-E
mrn@ncmrwf.gov.in gopal@ncmrwf.gov.in
National Centre for Medium Range Weather Forecasting

ABSTRACT

Simulation of Asian Summer Monsoon is still a challenging task even after 4 decades of efforts using numerical weather prediction techniques. Prediction of the strength of the Indian summer monsoon, its spatial behavior and the amount of precipitation is of great importance to Indian economy. Models incorporating complex surface processes including physically based descriptions of soils and vegetation have been developed since mid 1980s. When these models are coupled to general circulation models significant differences are reported due to land surface / atmosphere interactions in time scales ranging from days to several weeks. The influence of different land surface parameters like vegetation cover, snow cover, ice cover, soil moisture and albedo on atmospheric circulatory patterns have been investigated by many authors. Earlier studies experimenting with evapotranspiration at potential rate over dry surfaces in the interiors of large continents found that surface drying had little effect on precipitation rates in Southeast Asia and India. Further, over saturated land surface, changes in precipitation are directly related to changes in low-level moisture convergence associated with anomalous low-level flow. Over dry land surface, although low-level moisture convergence persists, it is unrelated to changes in tropical precipitation.

The T80/L18 GCM operational at National Centre for Medium Range Weather Forecasting, India incorporates a simple land surface scheme in which soil moisture evolution is simulated fixing the bucket capacity at 150 mm. By hindsight, it is incorrect to fix the bucket capacity through the model grid since the partitioning of sensible and latent heat fluxes may be prone to error. In the present work, we used variable bucket capacity over model grid incorporating GEWEX ISLSCP-II initiative "Global Soil Water Storage Capacity of the Rooting Zone" data to study the impact on Asian summer monsoon. The experiment is conducted for June 2004, the first month of Asian Summer Monsoon. The global data assimilation and forecasting scheme including analysis (spectral statistical interpolation) and forecast (T80/L18 with variable bucket capacity implementation) is run for each day to produce 5-day forecasts. Mean fields of analysis and 5-day forecasts are worked out for operational and experimental runs. Initial diagnostics suggested changes in low level circulatory patterns, partitioning of sensible and latent heat fluxes and rainfall. The RMSE and mean errors in temperature over Asian region showed marginal improvement. However, the improvements were significant over Europe and North America.

Key word: Root zone soil moisture, Asian Summer Monsoon, wind field, RMSE errors

1. Introduction

Models incorporating complex surface processes including physically based descriptions of soils and vegetation have been developed since mid 1980s (Dickinson 1984, Sellers et al.1986). When these models are coupled to general circulation models significant differences are reported due to land surface / atmosphere interactions in time scales ranging from days to several weeks. Shukla and Mintz (1982) compared the climate of a GCM with evapotranspiration at potential rate over dry surfaces in the interiors of large continents and found that surface drying had little effect on precipitation rates in Southeast Asia and India. Kerry and Anand (1991) investigated the effects of interactions between the tropical circulation and continental climate on the precipitation distribution by using idealized boundary conditions. They found that over saturated land surface, changes in precipitation are directly related to changes in low-level moisture convergence associated with anomalous low-level flow. Over dry land surface, although low-level moisture convergence persists, it is unrelated to the changes in tropical precipitation.

Soil moisture is one the most important components of the climate system. The summer drying phenomenon is a combination of the processes involving soil moisture, precipitation, time of snowmelt in the spring, partitioning of snowmelt into the soil or runoff, water table variations and potential evaporation due to warmer temperatures. Complex land parameterization schemes that incorporate biophysical control of evaporation have been developed over the time (BATS model – Dickinson et al. (1986), the Simple Biosphere (SiB) model – Sellers et al. (1986); Xue et al.(1991)). These schemes incorporate a large number of surface parameters. In NWP, the sensitivity to initial conditions prohibit their use in GCMs involving medium range weather prediction. These schemes are used with an advantage in long-term climate simulations (Pedro Viterbo, 2002).

The T80/L18 global data assimilation and forecast system operational at National Centre for Medium Range Weather Forecasting (NCMRWF) simulates the daily weather using

simple bucket model with a capacity of 150 mm of soil moisture. The disadvantage with fixed bucket scheme is that over very dry lands like sand deserts and over very wet lands like Amazon forest and other equatorial forest regions, partition of sensible and latent heat fluxes may be erroneous due to large deviation of fixed bucket value from the actual value. The magnitude of error in the partition of fluxes, in turn, show up in the simulation of soil wetness, In the present work, it is attempted to adapt variable bucket capacity over model grid for which the ISLSCP-II initiative Root Zone Water Storage Capacity (RZWSC) data derived using Photosynthetic ally Active Radiation (Kleidon and Heimann 1998) is used.

2. Design of the Experiment

The global data assimilation and forecasting system operational at NCMRWF comprises a global spectral model adapted from National Centers for Environmental Prediction(NCEP), USA. The model is implemented at T-80/L-18 resolution with intermittent data assimilation scheme involving spectral statistical interpolation (SSI) of Parrish and Derber (1992). In the assimilation cycle, 6-h forecasts of the global model are utilized to serve as first guess for subsequent analysis. Seven-day forecasts are produced daily on real time basis using 00UTC analysis.

The model uses a simple land-surface scheme that include (a) exchange coefficients computations based on Monin-Obukhov similarity theory with similarity functions of Businger et al. (1971) and Hicks (1976) as modified by Carson and Richards (1978) (b) Penman-Monteith method of evapotranspiration over land modified by Pan (1990) to include vegetation effects through stomatal resistance (c) prognostic surface temperature scheme of Arakawa (1972) (d) three layer scheme of Bhumaralkar (1975) for surface and soil temperature prediction (e) interactive bucket hydrology of Manabe (1969) for updating the soil moisture (f) evaporation over ocean by bulk method and (g) Charnocks roughness length computation over ocean.

The time dependent prognostic equations for estimation of surface temperature of Arakawa (1972) is:

$$\frac{\partial}{\partial t}(C_s \rho_s d_s T_s) = (1-\alpha) S\downarrow + L\downarrow - \sigma T_s^4 - H_o - LE_o - G - L_f E_x$$

where $(1-\alpha) S\downarrow$ is downward short wave radiative flux, α is the albedo, $L\downarrow$ is downward longwave radiative flux, σT_s^4 is upward longwave radiative flux at the surface temperature T_s,
where $H_o = - c_{pp} C_h(\theta (Z) - \theta (Z_o))$, $LE_o = \beta LE_p$ and β = fraction of soil moisture availability.

$$\beta = \begin{cases} 1 & \text{if } W > W_c \\ W / W_c & \text{if } W < W_c \end{cases}$$

where W is the available soil moisture, $W_c = 0.75 W_{fc}$, W_{fc} is the field capacity (=150 mm) and $L_f E_x$ is heat used for melting snow/ice.

Potential Evapotranspiration over land LE_p as given by Pan (1990):

$$LE_p = \frac{[(1-\alpha) S\downarrow + L\downarrow - \sigma T_a^4 - G] \Delta + (1-\gamma) LE_a}{\Delta + (1+\gamma)(1 + C_h \mid \vec{V} \mid r_s)}$$

where, σT_a^4 is upward longwave radiative flux at air temperature T_a,

$$LE_a = \rho L C_h \mid \vec{V} \mid (q_s(T_a) - q_a),$$

$$\Delta = \frac{L\, dq_s}{c_p dT} \quad \text{at } T_a \text{ and } \gamma = 4 \sigma T_a^3 / c_p C_h$$

The components of LE_a - the latent heat flux are:
ρ - density of air in the first model layer
L - latent heat constant of vaporization
C_h – turbulent exchange coefficient
V – Wind speed in the first model layer
$q_s (T_s)$ – saturation mixing ratio at surface temperature (skin temperature)
q_a – mixing ratio of air in the first model layer

The actual evapotranspiration is β times LE_p.

Excessive dryness of land surface with positive systematic error in surface temperature and lowered specific humidity at the first model layer have been recurring features of NCMRWF global model forecasts over the years. It is especially significant over north and central Indian regions.

By altering the size of the soil reservoir it was attempted to influence surface temperature and evaporation since evaporative fraction has a direct bearing on soil moisture availability and RZWSC in the formulation. Soil moisture is initialized by normalization as follows:

SOILM*(new_bucket_capacity)/(control_bucket_capacity)

The experiment is conducted for June, 2004 the first month of Asian Summer Monsoon.

3. Discussion and Results

The discussion is focused only on the Indian region due to space constraints although significant impacts are seen globally. We have a good idea on the performance of control T80 GCM; hence the experimental results are presented in comparison to control. RMSE and other scores are presented for different regions of the world to highlight the influence of RZWSC data on land surface processes.

The difference between RZWSC and operational bucket capacity is shown in Fig.1. All over the Indian region, RZMSC is higher except over NW arid regions where it is lower by about 100 mm. Along the west coast and over eastern reach of monsoon trough, RZWSC is very high ranging from 400 to 700 mm. The initial soil moisture in

experimental analysis (Fig.2) was very high nearing bucket capacity along Western Ghats during June 2004. Over NW arid regions the bucket fill was 100 mm less while over the rest of India it was 100 mm above control. Significant changes were seen over other parts of the world also. In the experimental analysis, stronger wind compared to control blew against northern parts of Western Ghats though the magnitude of raise in speed was low at less than 1 m/s (Fig.3). Anti-cyclonic bias over central parts of India and mild cyclonic tendency over northern parts of Western Ghats were other striking features.

In day-3 forecast (Fig.4), the converging Bay of Bengal branch of monsoon current blowing towards NE and adjoining regions had become stronger. The northern plains experienced westerly bias and the west coast, the gateway of SW monsoon current, exhibited cyclonic tendency by and large. Anti-cyclonic tendency over central parts prevailed at reduced magnitude.

Day-3 forecast rainfall (Fig.5) suggested an increase of 5-20 cm over NE region. West coast too experienced rise in rainfall but of low order. Heavy drop of the order of 5-15 cm was witnessed over central parts adjacent to monsoon trough.

Latent heat flux was decreased by 40 w/m**2 over central Indian region where anti-cyclonic tendency prevailed in day-3 forecast (Fig.7). Rise up to 30 w/m**2, indicating increased evaporation, featured over the whole of Bay of Bengal, north Indian ocean and Gujarat regions where merging of the monsoon current branches and cyclonic tendency were seen respectively. The NE region that experienced maximum boost in rainfall had witnessed marginal fall in latent heat flux below zero.

Day-3 forecast surface temperature (Fig.8) was rised by about 1.5 deg over central parts of India and parts of north India where eastern end of monsoon trough pass through. A fall of the order of -0.5 deg was experienced all over Gujarat and southernmost parts of India. Maximum fall of –1 deg was confined to a small pocket over Gujarat. It is interesting to note that the NE areas were subjected to marginal rise of 0.5 deg even though the total rainfall was amplified significantly. Mixed response was seen over oceans where the air temperature values were ranged between –0.5 to 0.5.

The rise and fall in the initial soil moisture over different parts of India had not diametrically influenced the forecast rainfall. In fact increased rainfall was seen over the drier regions in the experiment. Wetter regions did not coincide with increased rainfall activity consistently.

The RMSE errors against radiosonde data for two fields - temperature and wind - at 850-hPa level were shown in Fig.9 and Fig.10. In the legend, ‘A’ stands for Asia and ‘E’ stands for Europe. In the operational run, the error in forecast temperature increased from 2.4 deg. to 3.9 deg. from day-1 to day-5 forecast over Asia whereas the experimental run for the same region marginally reduced the error by 0.1 deg (Fig.9). Over Europe, the error in experimental forecast temperature was reduced by 0.2 to 0.5 deg. The most significant feature was that in the operational run, the errors over Europe were more pronounced than over Asia whereas experiment brought down the errors over Europe below the Asian values. The experiment did not bring about any change worth of consideration in the wind field RMSE errors over Asia and Europe (Fig.10).

4. Conclusions

a. Increased rainfall activity had resulted from magnified wind speed hitting against Western Ghats and convergence over north Bay of Bengal and adjoining NE region rather than due to increased soil moisture as evidenced from the marginally reduced latent heat flux.
b. There was no definite signal as to the influence of increased soil moisture on the simulation of Asian summer monsoon rainfall as both the regions of increased rainfall activity – the Western Ghats and the NE region – witnessed strong wind activity.
c. The global distribution RZMSC had discernible effect on the wind fields in simulating the Asian summer monsoon. Over central Indian region, the monsoon activity during June, 2004 was below normal resulting in poor rainfall. This feature was magnified in the experimental simulation leading to increased surface temperature and reduced latent heat. Thus, almost all the biases of operational forecast have magnified by the use of RZMSC data. No improvement in the spatial activity of Asian summer monsoon was brought out by the use of RZMSC.
d. Global distribution of RZMSC could not significantly influence the RMSE errors over tropics but showed significant improvement in RMSE errors over Europe and North America.

References

Arakawa, Tech.Rep **7,** 103, Dept. of Met, Univ.Cal , 1972.
Bhumaralkar, JAM, **14**, 1246, 1975.
Businger et al., JAS, **28**, 181, 1971.
Carson and Richards, BLM, **14**, 67, 1978.
Charnock, QJRMS, **81**, 639-648, 1955.
Dickinson, Amr.Geop.Uni Geophys. Monogr, **29**, 58, 1984.
Dickinson et al., NCAR/TN-275+STR, 69, 1986.
Hicks, QJRMS, **102**, 535, 1976.
Kerry and Anand, JC, **4**, 873-889, 1991
Kleidon and Heimann, Global change biology, **4**, 275-286, 1998.
Manabe, MWR, **97**, 739, 1969.
Pan , MWR, **118,** 2500, 1990.
Parrish and Derber, MWR, **120**, 1747-1763, 1992
Pedro Viterbo, Meteorological Training Course Lecture Series, 4, ECMWF, 2002.
Sellers et al. JAS, **43**, 505, 1986.
Shukla and Mintz, Science, **215**, 1498-1507, 1982.
Xue et al, JC, **4,** 345-364, 1991

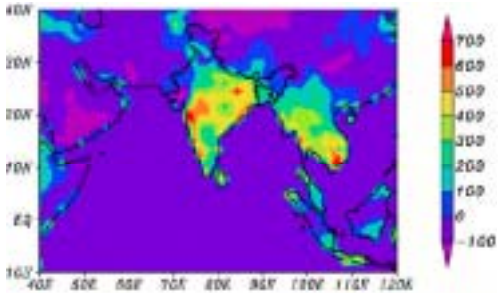

Fig.1 Difference between EXP and CTL Soil Reservoir Capacity (mm)

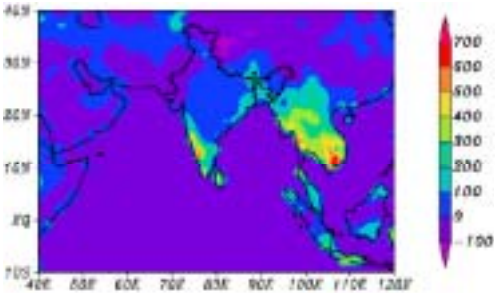

Fig.2 As in Fig.1 but for initial soil moisture for June 2004

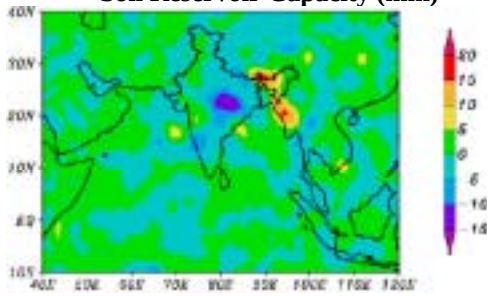

Fig.3 As in Fig.1 but for day-3 total forecast rainfall (cm) for June 2004

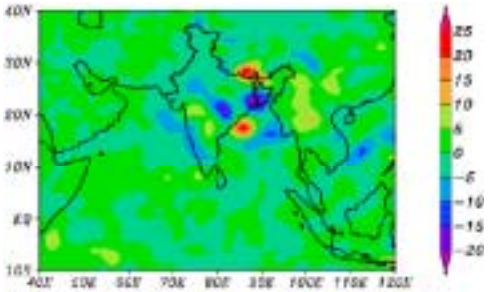

Fig.4 As in Fig.3 but for day-5 forecast

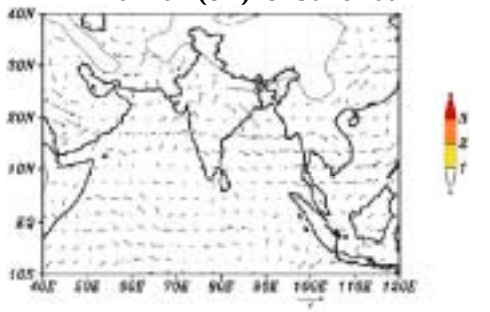

Fig.5 As in Fig.2 but for wind at 850 hPa

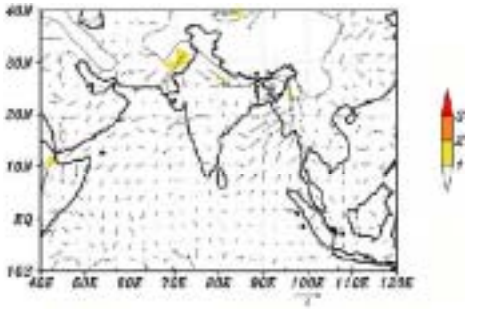

Fig.6 As in Fig.1 but for day-3 forecast

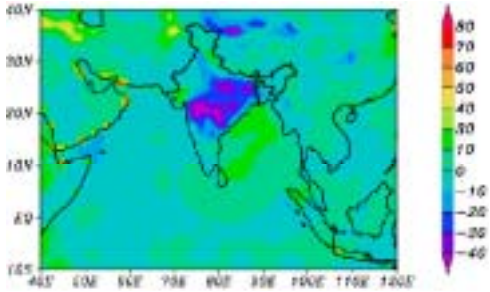

Fig.7 As in Fig.1 but for latent heat flux(w/m2)**

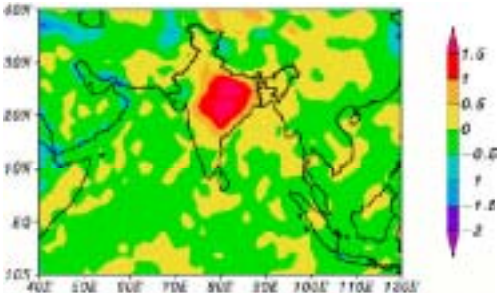

Fig.8 As in Fig.1 but for surface temperature

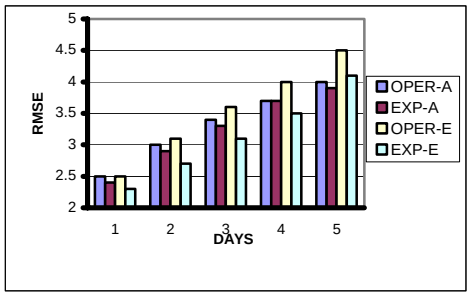

Fig.9 RMSE errors in temperature at 850 hPa

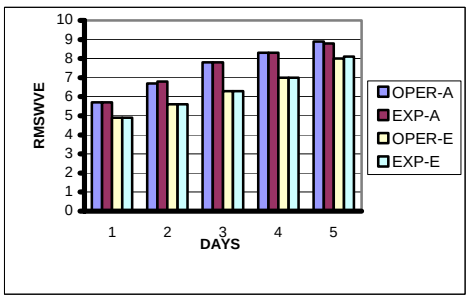

Fig.10 RMSE errors in wind at 850 hPa